# EFFECTS OF MULTIPLE-NOZZLE DISTRIBUTION ON LARGE-SCALE SPRAY COOLING VIA NUMERICAL INVESTIGATION

by

***Qiang XIE[a*], Zuobing CHEN[a], Gong CHEN[a,b], Yongjie YU[a], and Zheyu ZHAO[a]***

[a] School of Mechanical and Electronic Engineering, Wuhan University of Technology, Wuhan, Hubei, China
[b] Sinoma (Suzhou) Construction Ltd., Kunshan, Jiangsu, China

Original scientific paper
https://doi.org/10.2298/TSCI171223115X

*Spray cooling has been widely employed in many applications due to its high flux removal ability. A previous study has been conducted to reveal the large-scale spray cooling performance of an industrial used single nozzle. Continuously, influence of multiple-nozzle distribution has also been numerically investigated in present work. The mean heat flux and its standard deviation and uniformity are used to qualify the cooling performance. A flat wall with 1.6 m in length and 1.0 m in width has been taken as the research object. Effects of nozzle number, distance and offset have been parametrically compared. It is found that increasing nozzle number could promote mean heat flux, improve the uniformity of cooling patterns and enhance heat transfer performance. A best nozzle number of 10 could be obtained by an equation fitting. Decreasing nozzle distance turns out to be detrimental to heat transfer. The reason comes from the collisions and interactions of two too adjacent nozzles. Based on choices in real practice, two types of arrays i. e. perpendicular and skew array have been discussed and compared. It is concluded that the skew array could obtain higher heat flux with more uniform distribution.*

Key words: *multiple-nozzle distribution, large-scale, spray cooling, numerical investigation*

## Introduction

Due to fast heat-removal ability, spray cooling has been widely used in many applications such as electronic chip cooling [1] and alloy quenching in metallurgy [2]. Considerable studies including four main aspects as followed have been conducted for well understandings of spray cooling and its related topics.

Firstly on formation, spray cooling appears when liquid like water is atomized by specific devices such as nozzles into plenty of fine droplets which then impact a heated surface, spreading, forming a thin liquid film and evaporating [3] and secondly on spray cooling mechanisms. According to liquid boiling curves, four regimes have been discovered including single-phase liquid cooling regime and nucleate boiling regime with high fluxes at low temperatures and transition boiling regime and film boiling regime with relatively-low fluxes at relatively-high temperatures [4, 5]. Thirdly on quantification and prediction of spray cooling performance, many efforts have been spent by Rybicki and Mudawar [6] on building correlations in single phase regime, nucleate boiling regime, transition boiling regime and film boiling regime [7] on experimental and theoretical investigations. Summaries could be found in

* Corresponding author, e-mail:johnarmstrong@whut.edu.cn; qiangxie_whut@163.com

reference [2]. Lastly on spray cooling enhancement, one way is to improve cooling medium characteristics such as employing Nanofluids for instead [8, 9] and mixing surfactants in proper concentration [10]. Another way is to alter the heated surface structure like promoting surface roughness [11] and processing fins [12, 13] and other micro structures [14].

Here a typical application of spray cooling is given. Figure 1 shows a schematic of rotary drum spray cooler (RDSC) with direct-reduced iron (DRI) material in granular bed. It is always meters in diameter and tens of meters in length. The material will be cooled from 1400 K to about 500 K. It is a key equipment in rotary hearth furnace technique [15] for processing iron-containing wastes in steelworks. The cooling device before RDSC is called waterfall rotary drum cooler (WFRDC). Different with RDSC, water falls along, other than sprays to, the drum wall. Heat removes mainly by convection. Comparing with WFRDC, the RDSC has many advantages such as higher heat transfer performance, lower size and occupied area, less energy consumption and longer working life. Hence it is patented and has already applied in many DRI production-lines of steel-making industry in China.

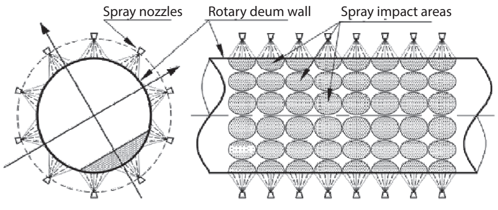

**Figure 1. Schematic of cooling system in spray cooling rotary drum**

During the design, operation, improvement and optimization of the RDSC, many practical problems have been encountered. For example when configuring spray system, the spray cooling performance needs to be evaluated conservatively at least and moreover, well understandings have to be established for effects of nozzle parameters such as nozzle number, nozzle distance and nozzle distribution. Even through the aforementioned studies have obtained some achievements, developed spray cooling technology and helped understanding fundamentals of spray cooling, their results cannot be directly introduced into the large-scale industrial application without any similarity criterions because they are on basis of laboratory-scale experiments on small surfaces. Anyway the spray system is so much different on large industry-scale RDSC.

The large-scale spray cooling for a single nozzle on RDSC has been numerically investigated [16]. Evaluation of spray cooling performance for single-nozzle becomes available. It is also revealed that the spray cooling performance on drum wall surface is almost same as that on a flat one when the wall curvature or the ratio of drum diameter to spray height is small [2]. Therefore, the drum wall could be unfolded to be flat for convenience. Figure 2 gives the schematic of flatten surface for drum wall in fig. 1. The heat dissipation flux shows different on different positions. Good nozzle configurations are strongly necessary to make relatively isothermal wall boundary in drum circumference direction.

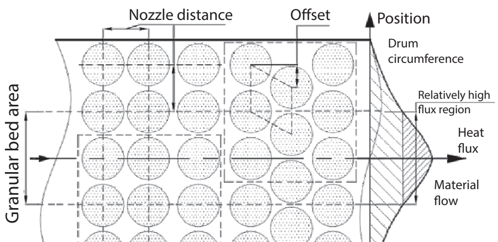

**Figure 2. Schematic of flatten surface based on drum wall along with its circumference; the circles with dots inside indicating spray impact areas; the nozzle distance, number and offset will be studied**

Based on the previous study [16], this work focuses on multiple-nozzle distributions like nozzle number and distance aiming to solve the nozzle configuration problems encountered in real practices. Efforts are made for creating new insights that will help guide, design, operate and optimize large-scale spray cooling applications.

## Model description

In present study the Euler-Lagrangian method is employed based on ANSYS Fluent package release 17.0 [17].

### Governing equations

The standard $k$-$\varepsilon$ model with time-averaged Navier-Stokes equations and standard wall functions as near-wall treatment is used. Governing equation details of the theory model are described in reference [16, 17].

In discrete phase, trajectories of droplets are controlled by the forces acting on them and the governing equations could be given in Lagrangian reference frame:

$$\frac{\mathrm{d}u_\mathrm{p}}{\mathrm{d}t} = F_D(u - u_\mathrm{p}) + \frac{\mathrm{g}\left(\rho_\mathrm{p} - \rho\right)}{\rho_\mathrm{p}} \tag{1}$$

in which is the drag for unit mass:

$$F_D = \frac{18\mu}{\rho_p d_p^2}\frac{C_D \mathrm{Re}}{24} \tag{2}$$

in which is dynamic drag coefficient:

$$C_D = \begin{cases} 0.424 & \mathrm{Re} > 1000 \\ \dfrac{24}{\mathrm{Re}}\left(1 + \dfrac{1}{6}\mathrm{Re}^{2/3}\right) & \mathrm{Re} \le 1000 \end{cases} \tag{3}$$

The droplets will follow three different laws including evaporation, inert heating and boiling based on varied thermal conditions. The droplet temperatures would be updated by the heat balance equation:

$$m_p c_p \frac{\mathrm{d}T_\mathrm{p}}{\mathrm{d}t} = hA_p(T_\mathrm{f} - T_\mathrm{p}) - \frac{\mathrm{d}m_p}{\mathrm{d}t}h_{fg} + A_p \varepsilon_\mathrm{p}\sigma\left(\theta_R^4 - T_p^4\right) \tag{4}$$

in which $h$ stands for heat transfer coefficient:

$$\mathrm{Nu} = \frac{hd_p}{k_\infty} = 2.0 + 0.6\mathrm{Re}_d^{1/2}\mathrm{Pr}^{1/3} \tag{5}$$

Coupling between the continuous phase and the discrete phase is considered. After the discrete enters into the continuous, the two-phases interact with each other in the aspects of mass, momentum and energy. The corresponding changes:

$$M = \frac{\Delta m_p}{m_{p,0}}\dot{m}_{p,0} \tag{6}$$

$$F = \sum\left\{\frac{18\beta\mu C_D \mathrm{Re}}{24\rho_p d_p^2}(u_p - u)\dot{m}_p \Delta t\right\} \tag{7}$$

$$E = \frac{\dot{m}_{p,0}}{m_{p,0}}\left[\Delta m_p\left(h_\mathrm{pyrol} - h_{fg}\right) + m_{p_{in}}\int_{T_\mathrm{ref}}^{T_{p_\mathrm{in}}} c_{p_\mathrm{p}}\,\mathrm{d}T - m_{p_\mathrm{out}}\int_{T_\mathrm{ref}}^{T_{p_\mathrm{out}}} c_{p_\mathrm{p}}\,\mathrm{d}T\right] \tag{8}$$

The typical SIMPLE algorithm is used for pressure-velocity coupling. During spatial discretization, a first order upwind scheme is employed for turbulent kinetic energy and dissipation rate, while a second order upwind scheme for momentum and energy.

### *Wall boundary of discrete phase*

Wall boundary of discrete phase is of much importance in simulating spray cooling on a wall surface. For spray-wall interaction, the wall-film boundary is applied. It is a specific boundary condition for simulation of liquid droplets colliding with walls and forming thin films, which is a proper choice for present study of spray cooling. The discrete phase model (DPM) particles are employed to model the wall-film. The model allows a single component liquid drop to impinge upon a boundary surface, form a thin film and do heat and mass transfer. Four main mechanisms are included in whole processes which are stick, rebound, spread, and splash according to impact energy and wall temperature. Figure 3 schematically shows the basic mechanisms considered for the wall-film model. Details of the wall-film model theory could be found in reference [17].

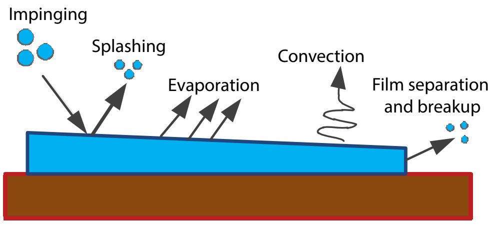


**Figure 3. Schematic of mechanisms in wall-film boundary theory**

### *Simulation conditions*

A flat wall with 1.6 m in length and 1.0 m in width is focused. The wall temperature keeps unchanged as 673 K. Figure 4(a) shows the system boundary conditions. Natural industry water in 283 K is served and sprayed by solid-cone pressure swirl nozzles which are widely used due to simple geometry and excellent atomizing performance [18]. The nozzle parameters include orifice diameter 2.0 mm, spray angle 60°, spray height 0.36 m, upstream pressure 0.6 MPa and flow rate 0.1 kg/s.

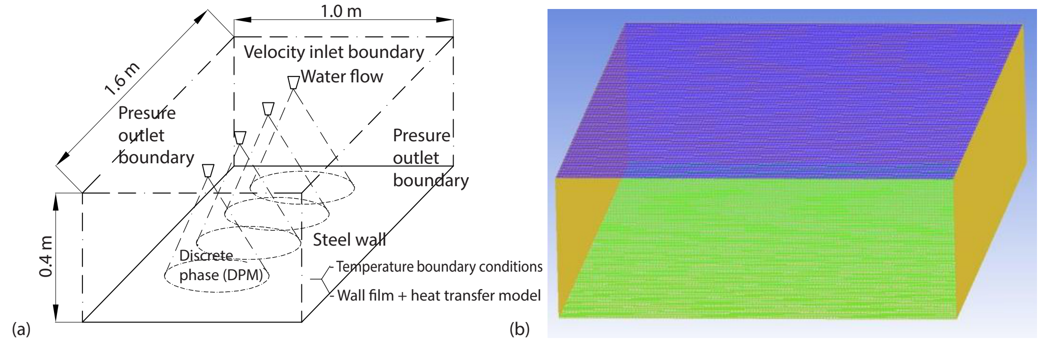


**Figure 4. (a) Schematics of the boundary conditions of simulated system (standard atmosphere) and (b) the computational mesh**

A structured mesh of 1475000 elements with local refinement in computational domain is employed, fig. 4(b). The grid convergence index (GCI) method explained by Roache [19] has been used to assure the mesh independence. The GCI is given:

$$GCI = \frac{F_s|\varepsilon|}{r^p - 1} \tag{9}$$

in which $F_s$ is safety factor with a suggested value 3.0 for comparison of two grids, $p$ – the order of convergence and has a numerical value of two, $\varepsilon$ and $r$ are, respectively, the relative error of solutions and the mesh refinement ratio ($r > 1$). The GCI needs to be determined at the least stable region in computational domain, which makes sure that mesh in other regions has little influence on results. The whole domain is chosen for convenience. Two cases with mesh refinement ratio as about 1.5 have been calculated and the mean heat fluxes are compared. The maximum GCI is approaching 4.8%. The small value indicates that the computational domain is already in mesh independence [19].

The transient computation proceeds by calculating firstly the continuous phase flow field. Then the DPM is introduced and its arguments like trajectory and velocity would be defined by coupling computing. The changes of mass, momentum and energy will be added as source terms into continuous phase flow. The whole computation ends until convergence occurs by monitoring the droplet flows and heat transfer processes.

## Results and discussions

The validity of the proposed numerical model for spray cooling has been demonstrated in our previous work [16]. Therefore, the model verification part has been omitted for concise. The heat transfer performance under different circumstances is focused in this work. In particular, the mean heat flux and its standard deviation (STD) and uniformity index on the wall surface are analysed after the simulations are converged.

The mean heat flux is calculated by computing the time average (mean) of the instantaneous values of heat flux. The STD is obtained using:

$$\sigma_{\overline{q}} = \sqrt{\frac{\sum_{x=1}^{n}\left(\overline{q_x} - \overline{q_a}\right)^2}{n}} \tag{10}$$

besides, the uniformity index of mean heat flux $\gamma_{\overline{q}}$ represents how the heat flux varies over the wall:

$$\gamma_{\overline{q}} = 1 - \frac{\sum_{x=1}^{n}\left[\left(|\overline{q_x} - \overline{q_a}|\right)A_x\right]}{2|\overline{q_a}|\sum_{x=1}^{n}A_x} \tag{11}$$

where $\overline{q_x}$ is the cell value of mean heat flux at each facet, $x$ – the facet index of the domain surface with $n$ facets, and $\overline{q_a}$ is the average value of $\overline{q_x}$ which is given:

$$\overline{q_a} = \frac{1}{n}\sum_{x=1}^{n}\overline{q_x} \tag{12}$$

The three augments as evaluation of heat transfer performance would be discussed in following sections.

### *Effect of nozzle number on spray cooling performance*

The nozzle number is an important configuration parameter of spray cooling system. Excessive nozzles would result in at least dense distributions, high nozzle costs and great risk of nozzle issues. On the other hand insufficient nozzles may lead to low overall heat transfer speed. Figure 5 gives the mean heat fluxes from 2-12 nozzles with increment as 2 nozzles. The row distance in 5(b)-5(f) keeps the same as 0.4 m while the column distance varies from each other to makes to nozzle arrangement more uniform. Figure 6 shows the variation of area-weighted average mean heat flux over nozzle number. As expected, increasing nozzle number would enhance the wall surface heat flux. The wall is wide enough and more nozzles obtain larger spray impact areas (heat transfer areas) and improve heat transfer performance. However since the wall has a limited area, the heat flux cannot rise all the time with more and more nozzles. The collisions between two nozzle sprays would become remarkable and influence each other resulting lower impact velocities and heat transfer rates, see figs. 5(e) and 5(f). It is inferred that excessive nozzles will result in bad spray cooling performance. The relationship between mean heat flux and nozzle number could be fitted well by $y = -463.2x^2 + 9702x + 2.46 \cdot 10^4$, which makes the optimum nozzle number close to 10. The result could give significant guidance in similar circumstances when designing spray cooling system.

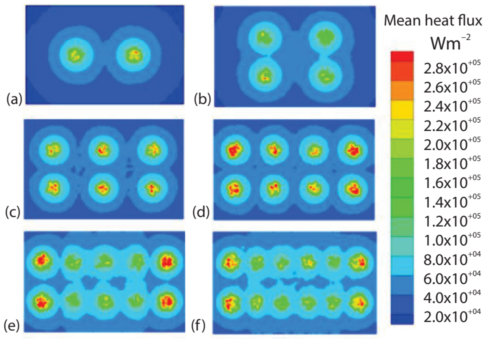


**Figure 5. Contours of mean heat flux under different nozzle numbers (2 to 12 nozzles with increment 2 nozzles are shown, respectively)**

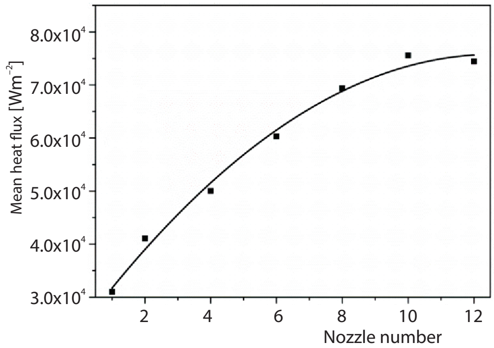


**Figure 6. Variation of area-weighted average mean heat flux on nozzle number; the solid line is fitted as $y = -463.2x^2 + 9702x + 2.46 \cdot 10^4$**

The STD of mean heat flux increases with nozzle number from 1-10 and then starts to decrease from 10-12. It should be noted that the STD rises a little from 2-4 nozzles while it improves dramatically from 4-10 nozzles, see fig. 7(a). The reason this difference should be the array change in rows and in columns. The uniformity index of mean heat flux increases at from 1-6 nozzles and then gradually decreases to 12 nozzles, see fig. 7(b). Improving nozzle arrangement promotes the impacting uniformity of spray droplets. However continually increasing nozzle number may reduce the uniformity due to the aforementioned remarkable collisions and disturbance between close sprays. The overall variation of uniformity is small (less than 7%) and the uniformity index cannot be well enough because of the non-uniformity essence in sprays.

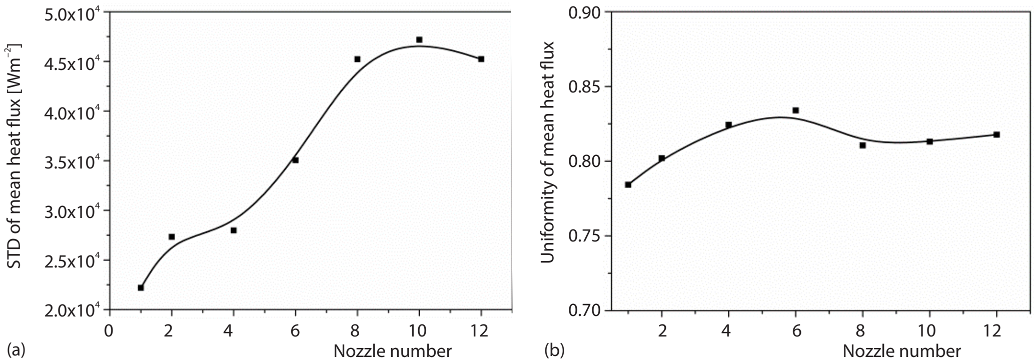


**Figure 7. Variation of standard deviation; (a) and uniformity (b) of mean heat flux over nozzle number**

### *Effect of nozzle distance on spray cooling performance*

The nozzle distance (ND) between 4 nozzles as two groups is discussed in this section. The row distance in each group keeps the same as 0.4 m while the distance in column changes. Figure 8 shows the contours of mean heat fluxes in different nozzle distances, in base case nozzle distance equals to 0.6 m, seen in fig. 5(b). When the column distance is 0.4 m, the nozzles locates on the four vertexes of a square, fig. 8(a). The heat flux distribution also shows similar as a square. When the column distance increases, the two groups of nozzles start to keep away from each other, fig. 8(b). The heat transfer patterns begin transforming into rectangles until the interaction between two groups disappears, fig. 8(d). Figure 9 shows the variation between mean heat flux and nozzle distance. It can be seen that the area-weighted average mean heat flux increases with nozzle distance. The relationship can be fitted well by an exponential equation which is given as $y = 53318 - 70087.43e^{-5.7x}$. The maximum value is about $5.33 \times 10^4$ W/m$^2$, no matter how great the distance is, which can be easily understood because once the distance is larger than a certain value, the two group nozzles cannot influence each other and the total heat flux would keep unchanged.

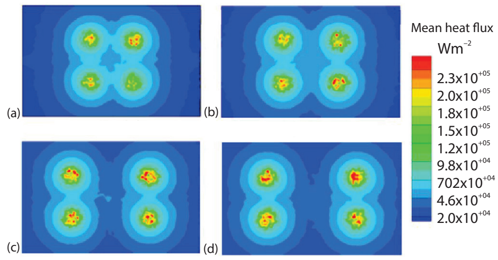


**Figure 8. Contours of mean heat fluxes under different nozzle distances; (a) ND = 0.4 m, (b) ND = 0.5 m, (c) ND = 0.7 m, and (d) ND = 0.8 m**

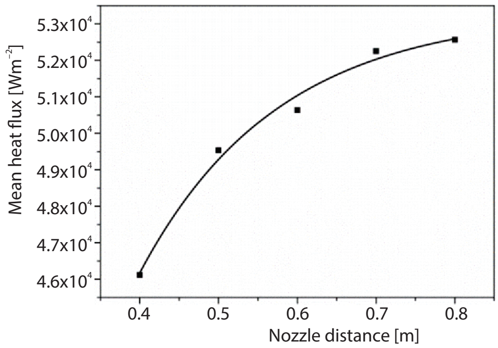


**Figure 9. Variation of mean heat flux on nozzle distance; the solid line is fitted as $y = 53318 - 70087.43e^{-5.7x}$**

Figure 9 shows the STD, fig. 9(a) and uniformity, fig. 9(b) of mean heat flux under different nozzle distances. The STD rises a little by 4.3% from $3.4 \cdot 10^4$ W/m$^2$ at 0.4 m to $3.17 \cdot 10^4$ W/m$^2$ at 0.5 m. Then decreases by 11.7% to $2.8 \cdot 10^4$ W/m$^2$ at 0.6 m. Then increases again. The uniformity keeps growing from 0.77 at 0.4 m to 0.82 at 0.6 m and then starts to reduce. The one peak changing demonstrates there is an optimum uniform distribution of heat flux in the simulated range. Based on data in two figures, it could be found that the STD and the uniformity of mean heat flux show best when the nozzle distance is 0.6 m. In a similar way, the variation keeps in a small range, less than 7%, indicating the non-uniformity nature in sprays shows prominent and cannot be ignored.

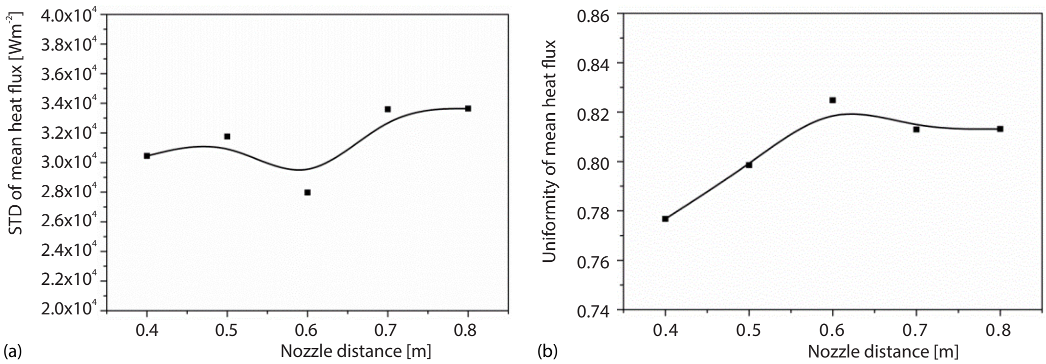


**Figure 10. (a) Variation of STD and (b) uniformity of mean heat flux on nozzle distance**

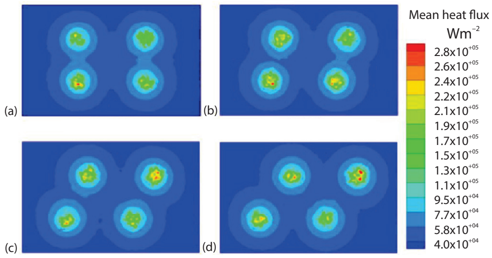


**Figure 11. Contours of mean heat fluxes under different nozzle offsets; (a) NOF = 0.0 m, (b) NOF = 0.1 m, (c) NOF = 0.2 m, and (d) NOF = 0.3 m**

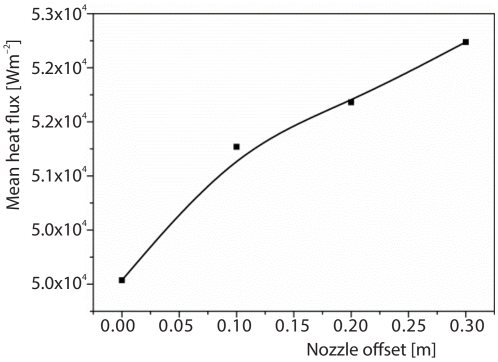


**Figure 12. The relationship between the mean heat flux and nozzle offset**

*Effect of nozzle offset on spray cooling performance*

Nozzle array has been turned out to be of much significance to heat transfer performance [20]. Two styles based on real practical choices are considered. One is perpendicular like the cases in former sections. Vertexes of adjacent nozzle positions constitute squares or rectangles. The other is skew. Vertexes of adjacent nozzle positions constitute parallelograms. Figure 11 shows heat transfer patterns under different nozzle offsets (NOF), definition in fig. 2. The case with nozzle offset 0.0 m refers to perpendicular nozzle arrangement while the other three cases are skew arrangement. The mean heat fluxes are compared in fig. 12. It could be found that when nozzle offset grows, the spray cooling performance continually improves, even though the amount of increase is limited about 4.4%.

The corresponding STD, fig. 13(a) and uniformity, fig. 13(b) of mean heat fluxes have been recorded. The STD increases by about 16% from nozzle offset 0.0 to 0.1 m and then it starts to weaken with small amount, 2.6%. The uniformity reduces a little from nozzle offset 0.0 to 0.1 m and then gradually rises to 0.82 at nozzle offset 0.3 m. The amount of increase of uniformity is, however, small because of not only the aforementioned non-uniformity essence of sprays but also a special nozzle position. For example, in fig. 11(d) when the nozzle offset equals to 0.3 m, three nozzles including two in the first row and the right one in the second form a good distribution, which helps improving uniformity of heat flux. However, presence of the last nozzle weakens this help. Even so, it can be inferred that the simulation results would be more prominent if the first three nozzles are employed. Anyway, compared with perpendicular arrangement, the skew one could obtain larger heat flux, better uniformity and more outstanding spray cooling performance.

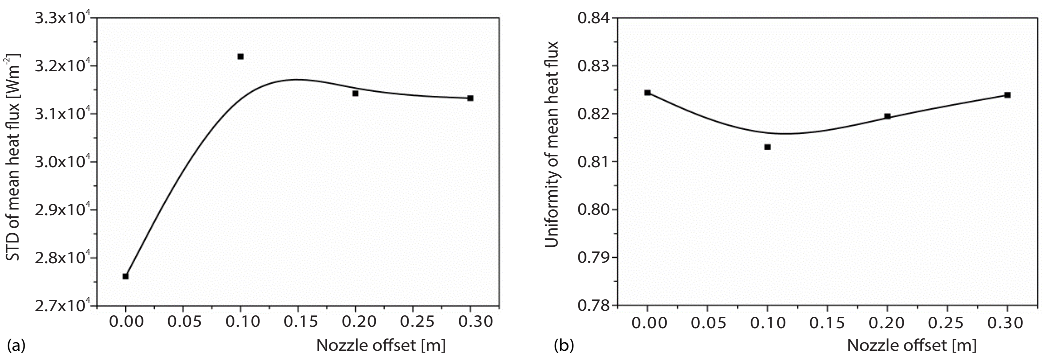


**Figure 13. (a) The STD and (b) uniformity of mean heat flux under different nozzle offsets**

## Conclusions

Effect of nozzle arrangement has been investigated via numerical simulations. Parametric studies have been carried out on three aspects including different nozzle numbers, different nozzle distances and different nozzle offsets. The mean heat flux and its STD as well as uniformity on the wall surface have been used to evaluate the spray cooling performance. It is found that increasing nozzle number could promote the heat flux and improve its uniformity. An optimum nozzle number is found by a fitting equation for the simulated wall surface. With nozzle distance reducing, collisions and interaction between adjacent nozzles become significant which is not helpful for improve heat transfer rate. Based on the simulated results, a proper distance is discovered to be good to both spray cooling performance and uniformity of heat transfer patterns. The skew nozzle array is proved to obtain higher heat flux and get better uniformity than perpendicular nozzle array.

All the simulated results are based on problems in real practices of RDSC. The findings are meaningful and useful for the designing, running, operating and optimization of the equipment. They also show much guidance to similar spray cooling system.

## Acknowledgment

The China Scholarship Council (CSC) (No. 201406950059) and the Enterprise cooperative Project of Wuhan University of Technology (No. WHUT-20162h0149) are gratefully thanked for financial support of this work.

## Nomenclature

$E$ – heat energy, [J]
$C_D$ – drag coefficient, [–]
$d_p$ – particle diameter, [m]
$F$ – force on particle in control volume, [kgms$^{-2}$]
$h_{fg}$ – latent heat, [Jkg$^{-1}$]
$k$ – thermal conductivity, [Wm$^{-1}$K$^{-1}$]
$M$ – particle mass change in control volume, [kgs$^{-1}$]
$\dot{m}_p$ – mass-flow rate of particles, [kgs$^{-1}$]
$\dot{m}_{p,0}$ – initial particle mass-flow rate, [kgs$^{-1}$]
$m_{p,0}$ – initial mass of particle, [kg]
$\Delta m_p$ – mass change of a particle as it passes through each control volume, [kg]
Pr – Prandtl number of continuous phase, [–]
Re – relative Reynolds number, [–]
$T$ – temperature, [K]
$\Delta t$ – time step, [s]
$u$ – fluid velocity, [ms$^{-1}$]

*Greek symbols*

$\varepsilon$ – emissivity, [–]
$\mu$ – molecular viscosity of the fluid, [kgm$^{-1}$s$^{-1}$]
$\rho$ – density, [kgm$^{-3}$]
$\sigma$ – Stephen Boltzmann constant, [Wm$^{-2}$K$^{-4}$]

*Subscripts*

f – continuous fluid phase
p – particles /droplets

## References

[1] Cader, T., *et al*.,Spray Cooling Thermal Management for Increased Device Reliability, *IEEE Transactions on Device and Materials Reliability*, *4* (2005), 4, pp. 605-613
[2] Mascarenhas, N., Mudawar, I., Analytical and Computational Methodology for Modelling Spray Quenching of Solid Alloy Cylinders, *International Journal of Heat and Mass Transfer*, *53* (2010), 25-26, pp. 5871-5883
[3] Horacek, B., *et al*., Single Nozzle Spray Cooling Heat Transfer Mechanisms, *International Journal of Heat and Mass Transfer*, *48* (2005), 8, pp. 1425-1438
[4] Liang, G., Mudawar, I., Review of Spray Cooling – Part I: Single-Phase and Nucleate Boiling Regimes, and Critical Heat Flux, *International Journal of Heat and Mass Transfer*, *115* (2017), Part A, pp. 1174-1205
[5] Liang, G., Mudawar, I., Review of Spray Cooling – Part II: High Temperature Boiling Regimes and Quenching Applications, *International Journal of Heat and Mass Transfer*, *115* (2017), Part A, pp. 1206-1222

[6] Rybicki, J. R., Mudawar, I., Single-Phase and Two-Phase Cooling Characteristics of Upward-Facing and Downward-Facing Sprays, *International Journal of Heat and Mass Transfer*, *49* (2006), 1, pp. 5-16
[7] Klinzing, W. P., *et al*., Film and Transition Boiling Correlations for Quenching of Hot Surfaces with Water Sprays, *Journal of Heat Treating*, *9* (1992), 2, pp. 91-103
[8] Hsieh, S.-S., *et al.*, Nanofluid Spray Heat Transfer Enhancement, *International Journal of Heat and Mass Transfer*, *94* (2016), Mar., pp. 104-118
[9] Wen, D., *et al*.,Review of Nanofluids for Heat Transfer Applications, *Particuology*, *7* (2009), 2, pp. 141-150
[10] Cheng, W., *et al.*, An Experimental Investigation of Heat Transfer Enhancement by Addition of High-Alcohol Surfactant (HAS) and Dissolving Salt Additive (DSA) in Spray Cooling, *Experimental Thermal and Fluid Science*, *45* (2013), Feb., pp. 198-202
[11] Zhang, Z., *et al*., Experimental Investigation of Spray Cooling on Flat and Enhanced Surfaces, *Applied Thermal Engineering*, *51* (2013), 1-2, pp.102-111
[12] Xie, J. L., *et al*., Study of Heat Transfer Enhancement for Structured Surfaces in Spray Cooling, *Applied Thermal Engineering*, *59* (2013), 1-2, pp. 464-472
[13] Silk, E. A., *et al*., Spray Cooling of Enhanced Surfaces: Impact of Structured Surface Geometry and Spray Axis Inclination, *International Journal of Heat and Mass Transfer*, *49* (2006), 25, pp. 4910-4920
[14] Sodtke, C., Stephan, P., Spray Cooling on Micro Structured Surfaces, *International Journal of Heat and Mass Transfer*, *50* (2007), 19-20, pp. 4089-4097
[15] Ichikawa, H., Morishige, H., Rotary Hearth Furnace Process for Steel Mill Waste Recycling and Direct Reduced Iron Making, *Revue De Metallurgie*, *100* (2003), 4, pp. 349-354
[16] Zuobing, C., *et al*., Numerical Simulation of Single-Nozzle Large-Scale Spray Cooling on Drum Wall, *Thermal Science*, *22* (2018), 1A, pp. 361-372
[17] ***, Inc, A., ANSYS Fluent Theory Guide, http://www.ansys.com
[18] Liu, X., *et al*., Flow Characteristics of Liquid Nitrogen through Solid-Cone Pressure Swirl Nozzles, *Applied Thermal Engineering*, *110* (2017), Suppl. C, pp. S290-S297
[19] Roache, P. J., Perspective: A Method for Uniform Reporting of Grid Refinement Studies, *Journal of Fluids Engineering*, *116* (1994), 3, pp. 405-413
[20] Sadafi, M. H., *et al*., Nozzle Arrangement Effect on Cooling Performance of Saline Water Spray Cooling, *Applied Thermal Engineering*, *105* (2016), July, pp. 1061-1066

Paper submitted: December 23, 2017
Paper revised: March 9, 2018
Paper accepted: March 12, 2018